

**HF Propagation Measurement
Techniques and Analyses**
ARRL and TAPR 39th Annual
Digital Communications Conference
September 11-12, 2020 – Virtual Online

Steve Cerwin WA5FRF

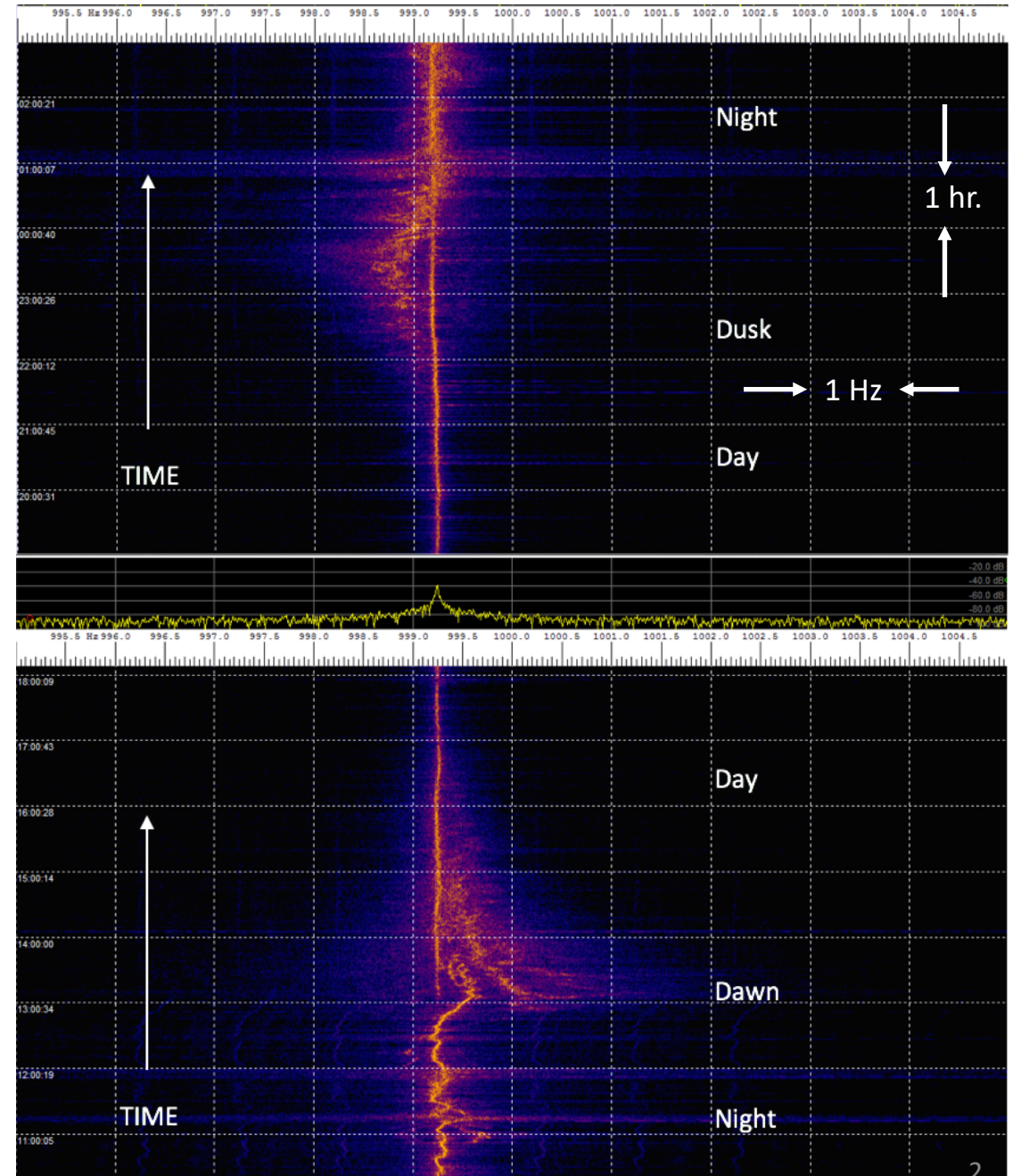
WA5FRF@arrl.net

Mico, TX 78056 EL09nn

N29' 35" W98' 53"

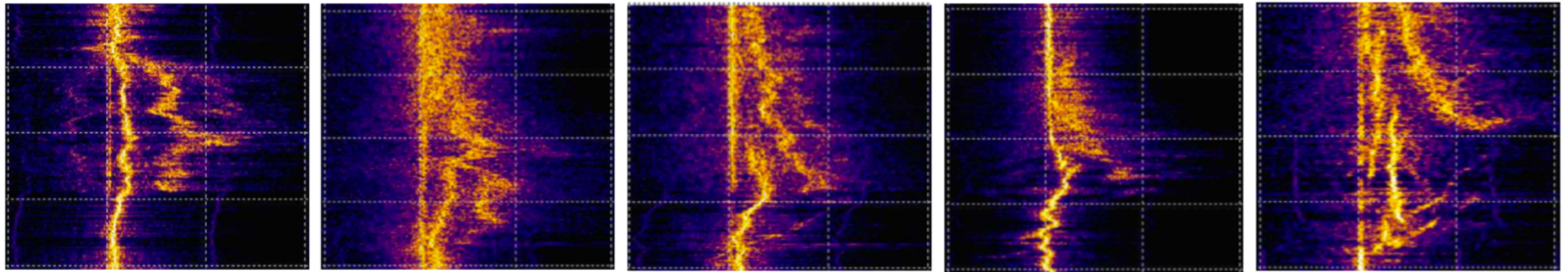
Motivation: Learn More About Ionospherically Induced Frequency Variations

On-Air Spectrograms of 5 MHz WWV Showed Smooth Daytime and Turbulent Nighttime Characteristics with a Prominent Negative Swing at Dusk and Positive Swing at Dawn. The Dawn Swing Additionally Showed Multiple Higher Order Swings, that Sometimes Manifesting Abruptly Mid-transition

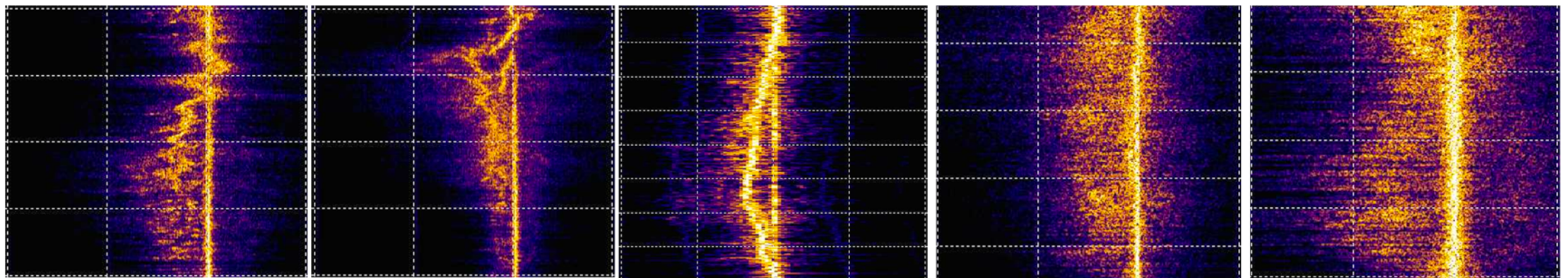


Mode Splitting Observed on WWV During Dawn and Dusk Transitions

Positive Frequency Excursions During Sunrise



Negative Frequency Excursions During Sundown

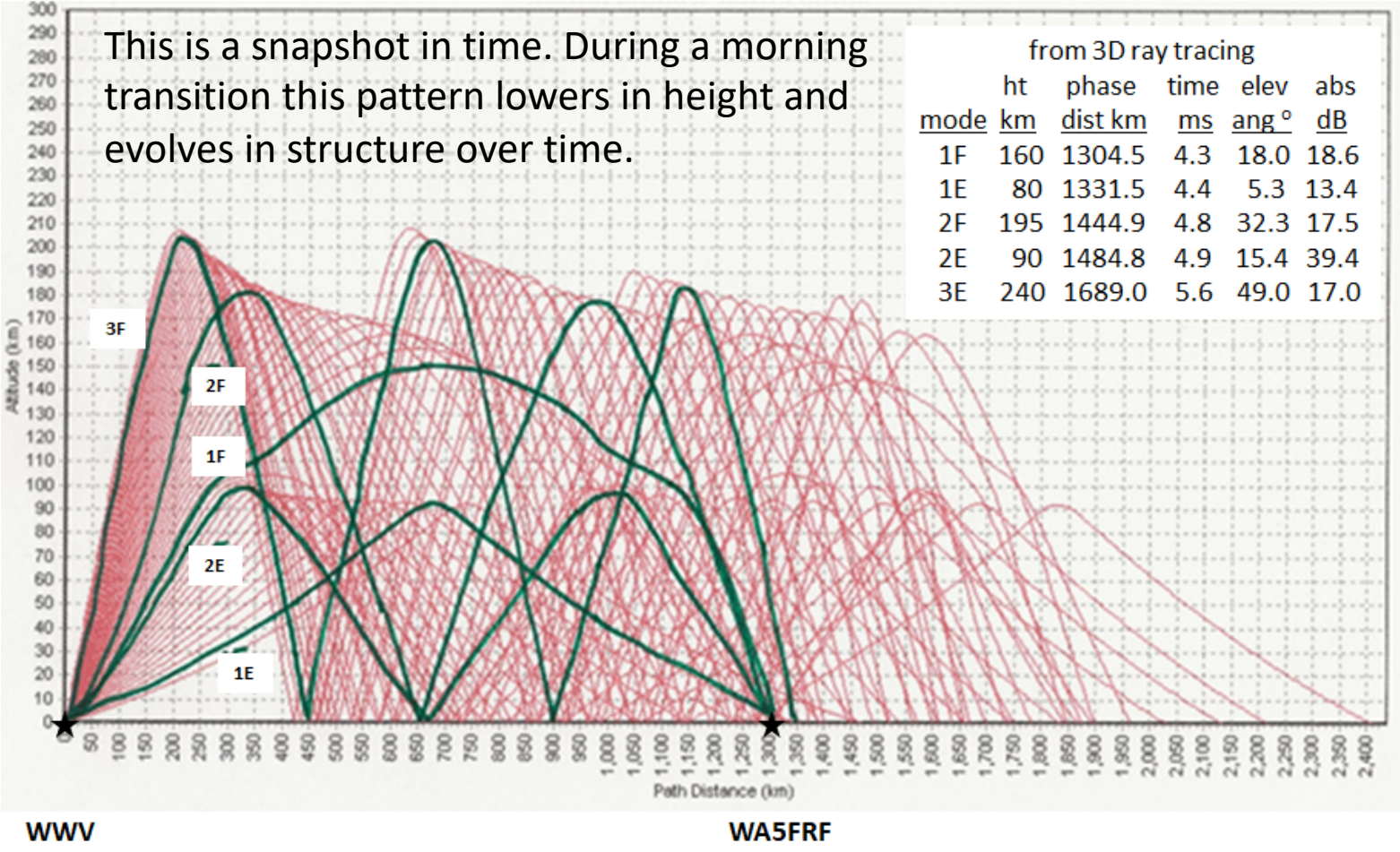


Ray Trace Simulation Predicting Multiple Propagation Modes from WWV to WA5FRF After Sunup

Postulated mode splitting mechanisms:

1. For multiple modes returning from a common layer, total path length increases according to number of hops. The longer modes close faster for a given layer descent speed, resulting in more Doppler shift according to number of hops.
2. Multiple hop modes that manifest abruptly do so when the required high angle of propagation is supported.
3. Bill Engelke AB4EJ suggested different Doppler tracks for simultaneous refractions from different layers.
4. Bill Liles WQ6Z suggested changing wave speed can be responsible for producing frequency shifts.

2D Ray Trace from WWV to WA5FRF, 4-50° in 1° steps, January 2020 at 1430 UTC on 5 MHz



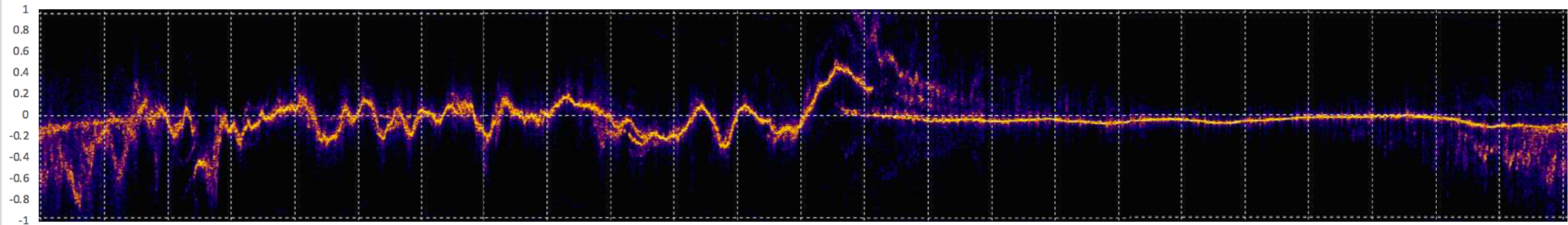
Simulation Provided by Carl Luetzelschwab K9LA

Measurement Tools and Techniques to Unravel Multiple Processes by Specific Testing

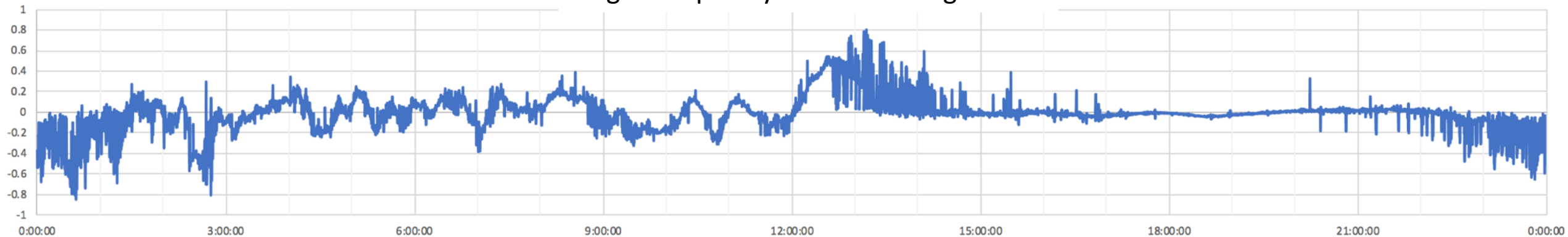
- Method to obtain high resolution frequency data: offset receiver low in frequency in USB mode to down convert the RF carrier to an audio tone. This preserves small frequency variations on that can be analyzed on a sound card spectrum analyzer or an audio frequency demodulator. A GPSDO provides atomic clock accuracy and stability.
- Compare simultaneous WWV spectrograms across multiple frequencies.
- Compare oscillographic time domain presentations of a GPSDO stabilized tone to the down-converted WWV carrier for study of short term amplitude and frequency variations.
- Measure Times of Flight of multiple modes using WWV per-second timing ticks and GPSDO synchronization to deduce propagation modes. Correlate data with ray trace simulations using actual solar-terrestrial data.
- Separate simultaneous WWV and WWVH spectrogram data by deinterlacing the 500 and 600 Hz side tone encoding.

Comparison Between Spectrogram and Single Frequency Formats During HamSCI Festival of Frequency Measurements

Spectrogram Format using Spectrum Lab



Single Frequency Detector using FLDIGI



Dusk Transition ----- > Night ----- > Dawn Transition ----- > Day ----- > Dusk Transition

Path: WWV, Ft. Collins CO to WA5FRF, near San Antonio, TX 0000z – 2359z October 1, 2019

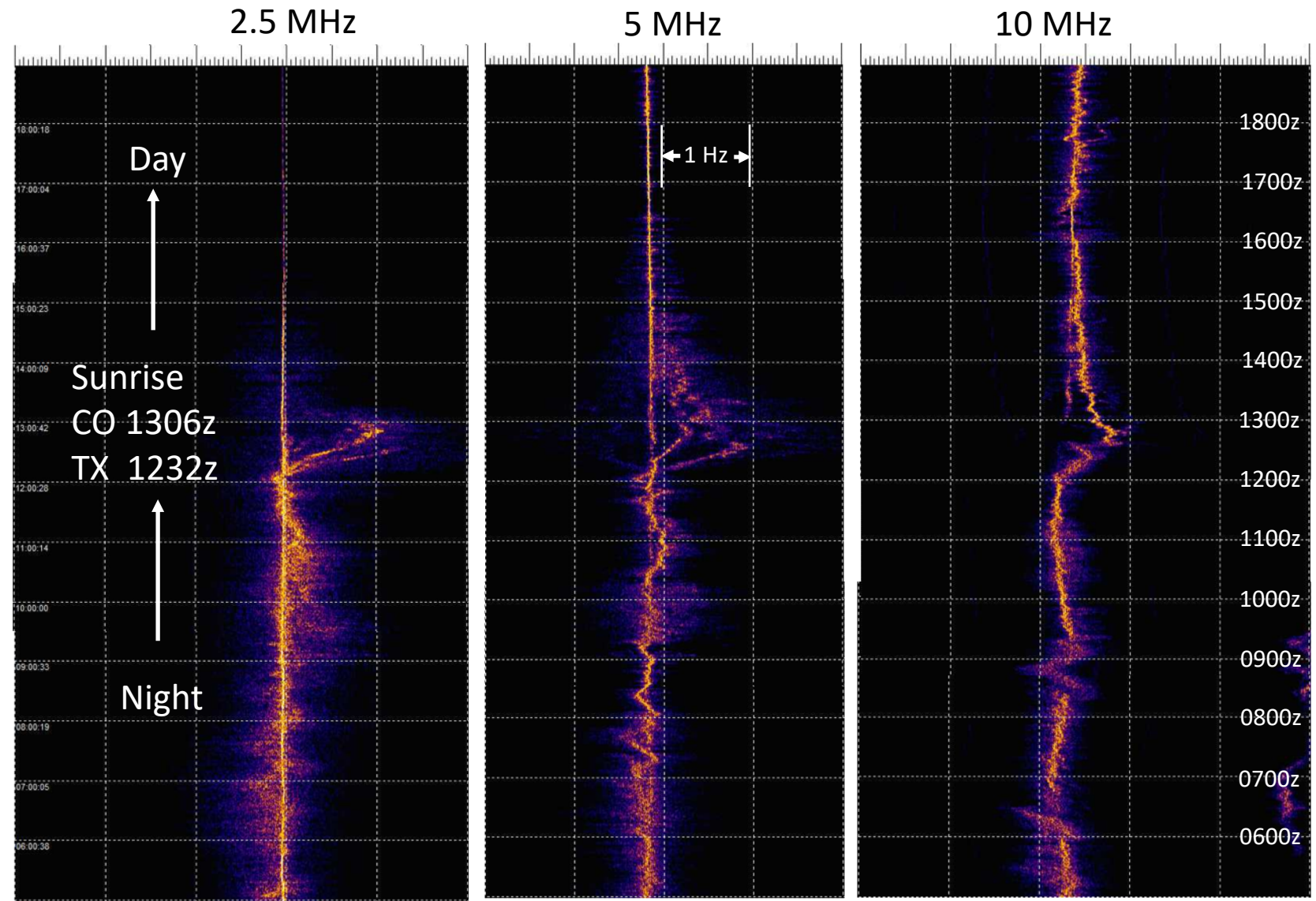
Simultaneous WWV Spectrograms at 2.5, 5, and 10 MHz During Dawn Transition

2.5 and 5 MHz frequency steady during the day and turbulent at night. 10 MHz frequency turbulent both day and night. Only weak correlation over frequency during turbulence. The turbulence amplitude does not scale with carrier frequency.

2.5 and 5 MHz manifest multiple high order modes during sunrise but 10 MHz does not.

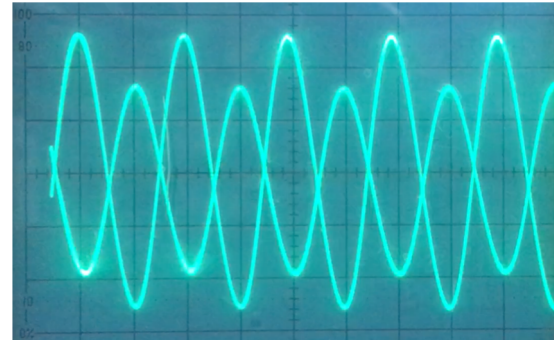
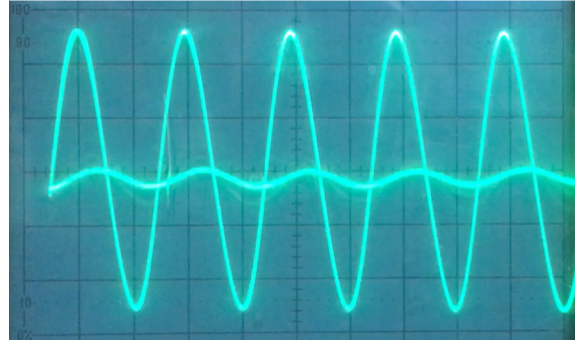
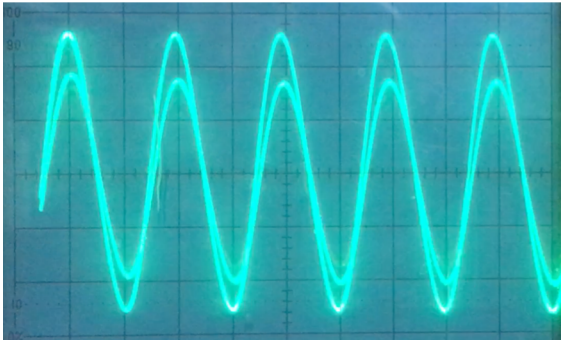
Some modes manifest or extinguish abruptly mid-transition.

All frequencies show a simultaneous mode showing little frequency shift.



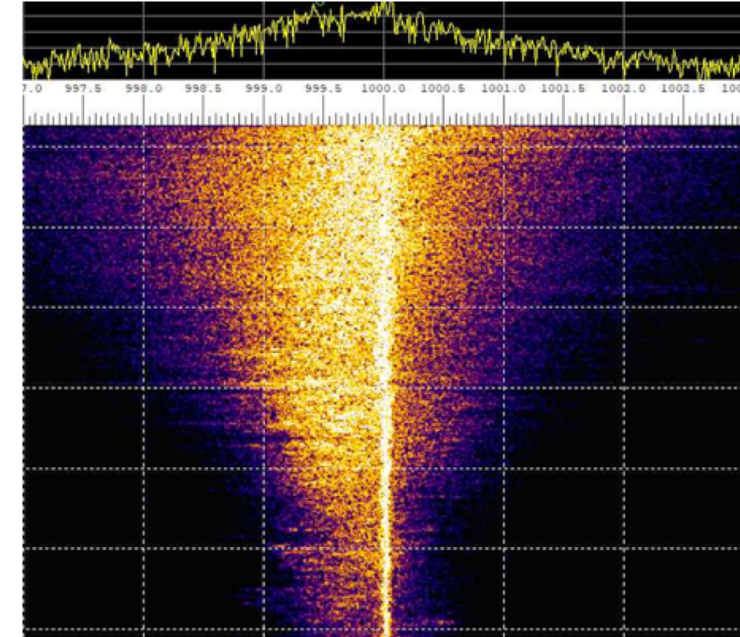
Ft. Collins, CO (40.68, -105.04) to San Antonio, TX (29.57, -98.89) on October 11, 2019 GPSDO on 2.5 MHz receiver only.

Time Domain Video Displays for Analysis of Short Term Variations



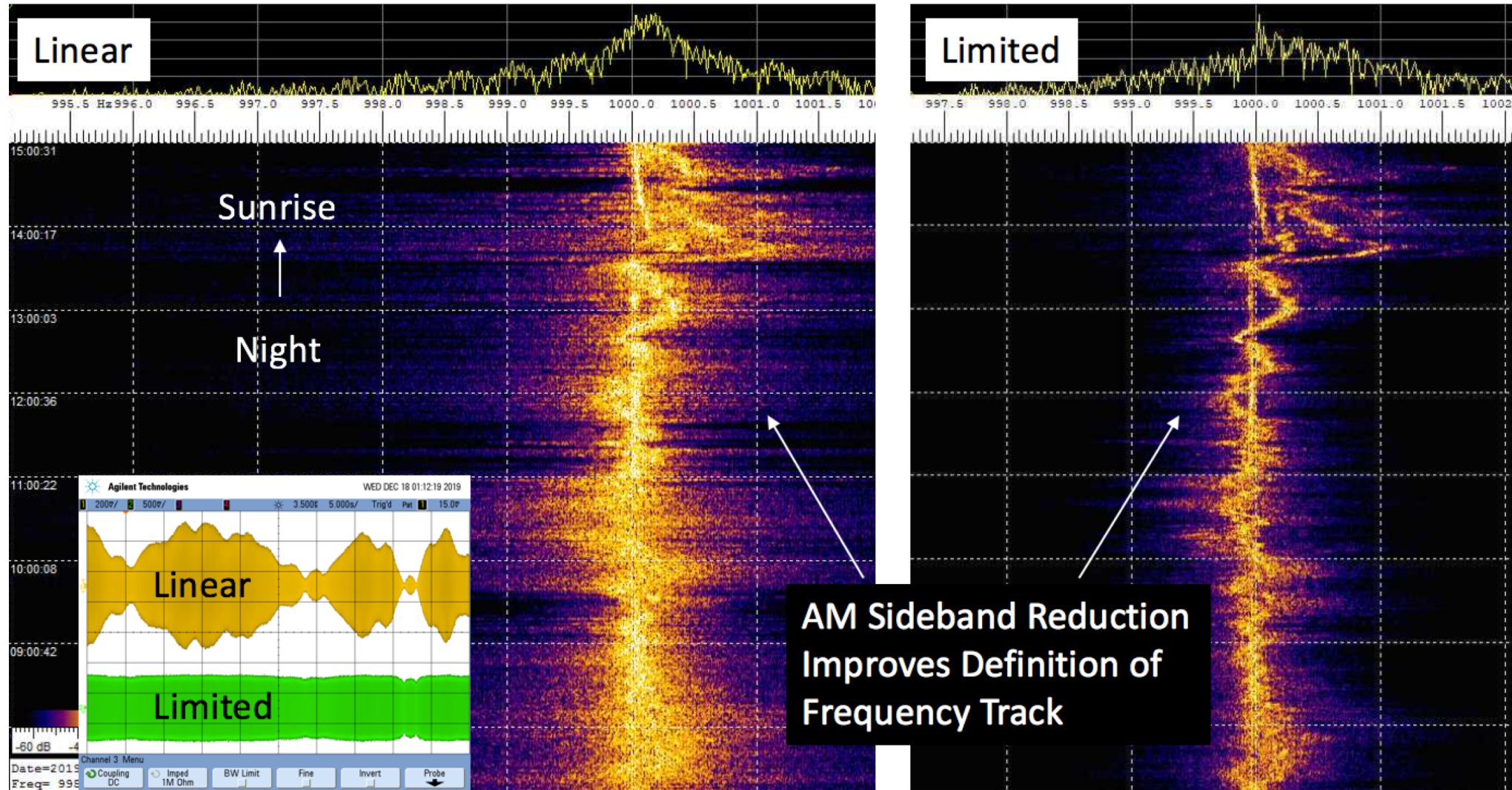
Rapid in-phase, null, and out-of-phase sequence occurring in less than 100mS

- Two 1 kHz tones with atomic accuracy and stability: A GPSDO stabilized function generator and on-air 5 MHz WWV downconverted to 1 kHz and filtered to 10 Hz bandwidth. The difference is that WWV arrived by skywave.
- This type of comparison in the time domain succinctly demonstrates AM and FM modulations imposed by the ionosphere during skywave propagation.
- Observed behavior includes steady amplitude with little frequency variation, rapid amplitude flutter with frequency shifts on the order of Hertz, and even larger amplitude fluctuations that include complete carrier nulls with phase reversals.
- Rapid and deep amplitude fluctuations can be considered a modulation process that can superimpose modulation sidebands on spectrograms.

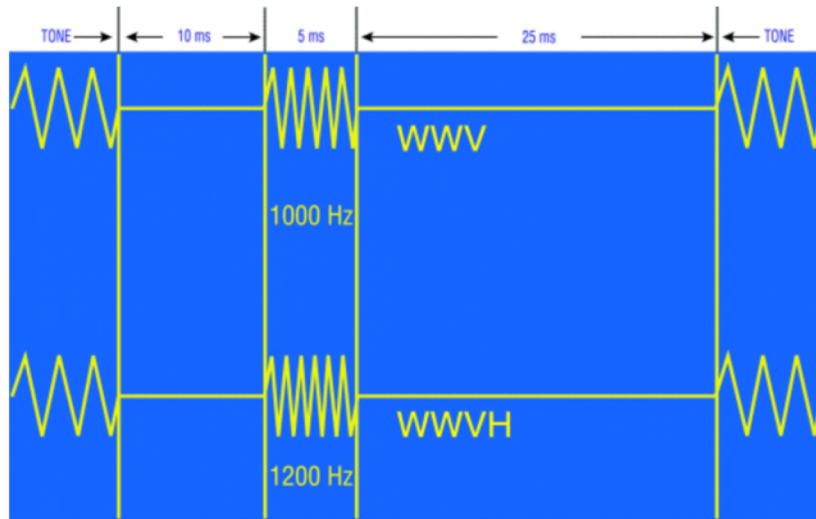


Spectrogram Showing Symmetrical Frequency Spread Suggestive of Modulation Sidebands

Passing Downconverted Carrier Through a Hard Limiter Sharpened Spectrogram by Stripping Amplitude Information

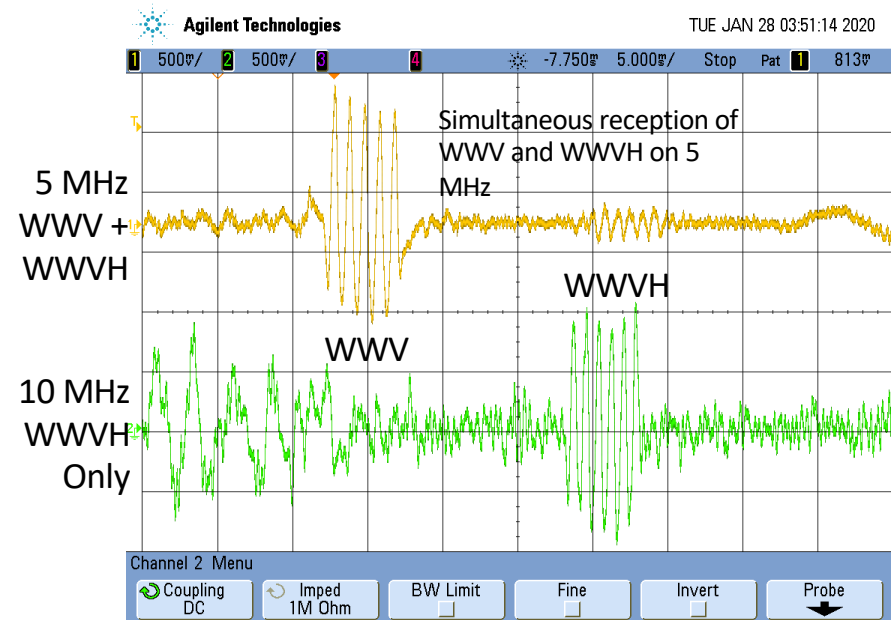


Time of Flight Measurements Using WWV Per-Second Timing Ticks



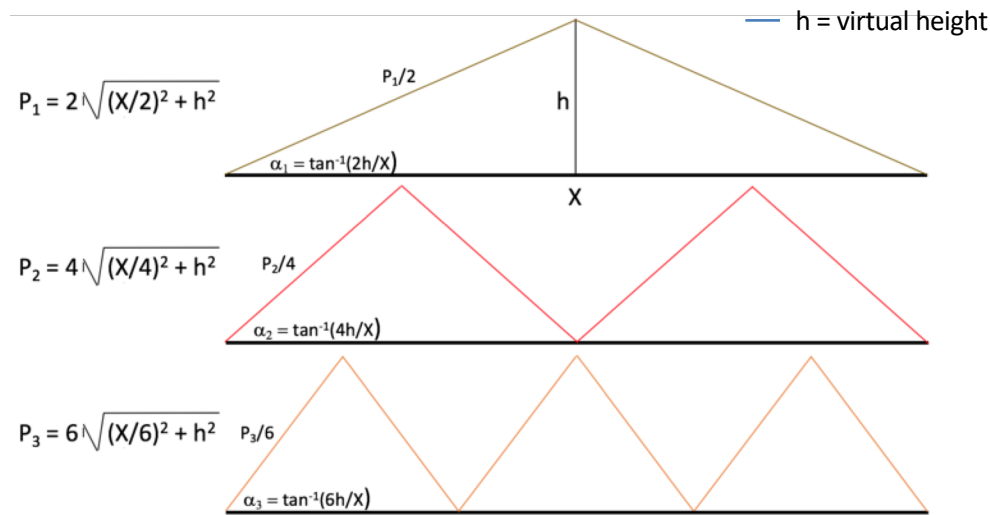
Published Timing Tick Information:
WWV – 5 cycles of 1000 Hz
WWVH – 6 cycles of 1200 Hz
Alternating 500/600 tone frequencies

A sync reference can be obtained from the 1 pps output from a GPSDO.



On-the-air reception of WWV and WWVH Timing Ticks
At WA5FRF. Time difference of arrival is ~17mS.
WWV at 1350 km, WWVH at 6050 km great circle dist.

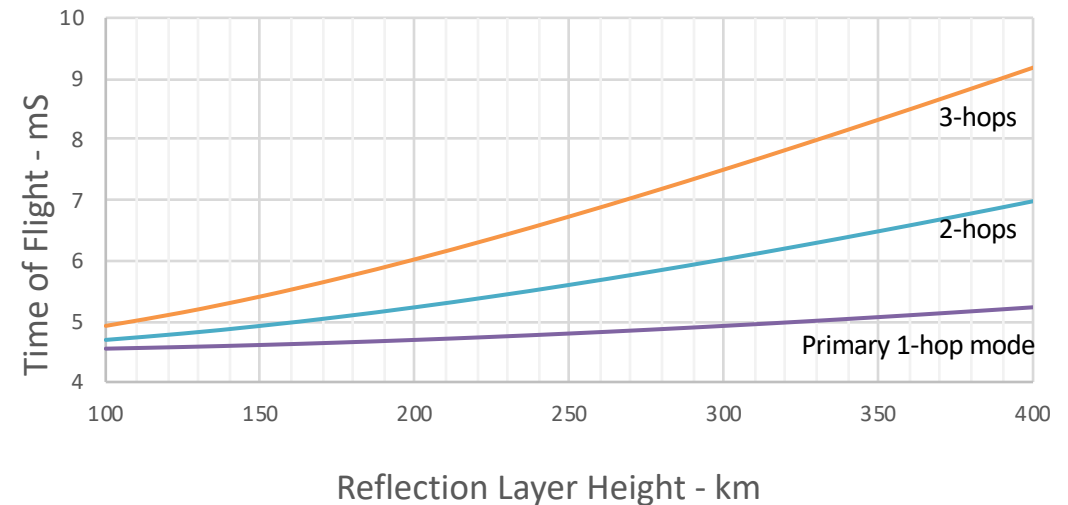
Idealized Geometry for 1, 2, and 3 Hop Paths Used to Approximate Expected Pulse Timing



Simplifications:

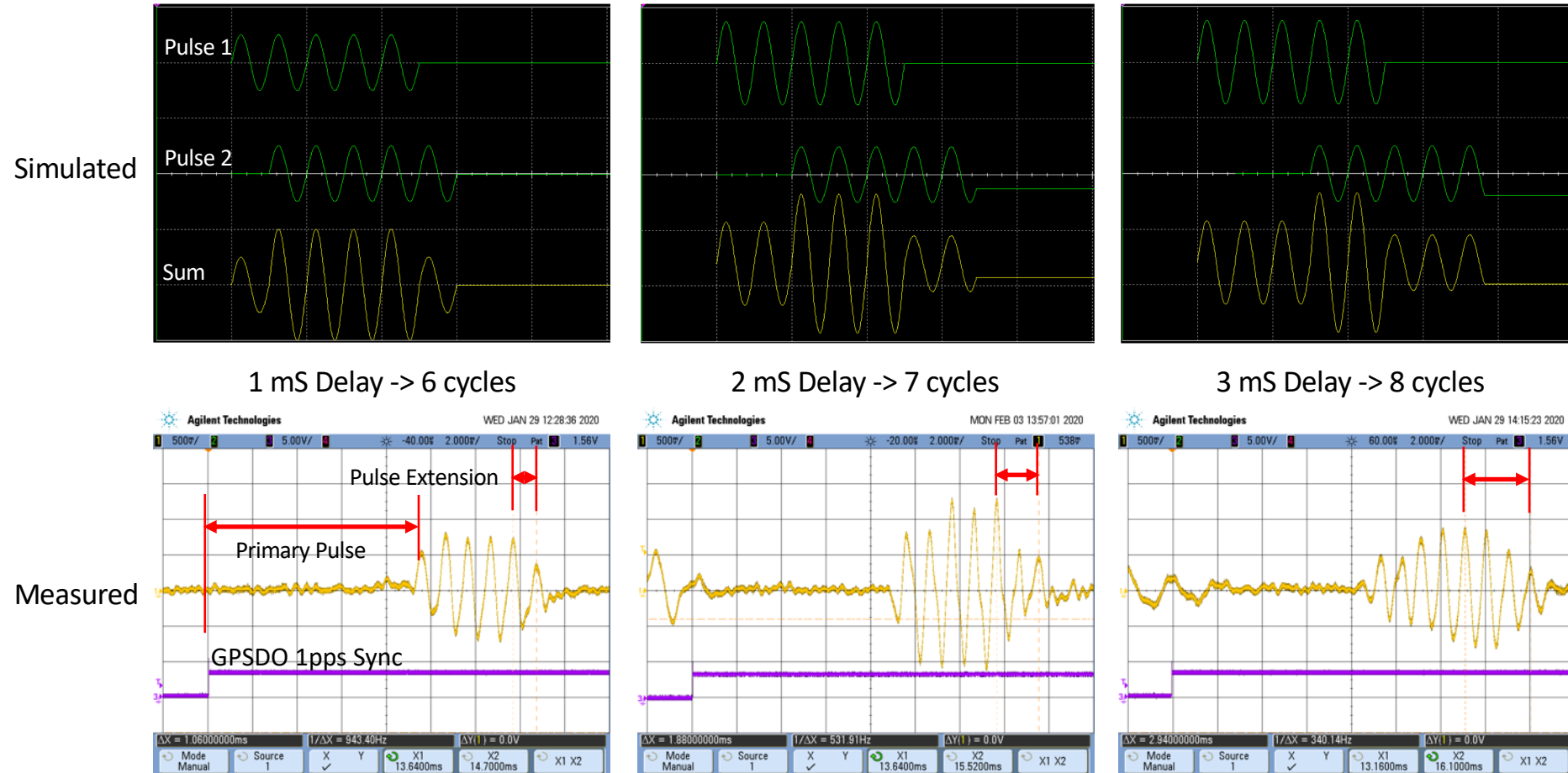
1. "Flat Earth" 2D geometry
2. Perfect reflections at constant virtual height
3. Constant wave speed = c

Geometric Times of Flight for 1, 2, and 3 Hop Paths from WWV to WA5FRF vs. Reflection Layer Height



For ground distance (X) of 1350km and reflection heights (h) from 150-300km, the differences in arrival times between the 1 and the 2 & 3 hop modes range from 0.3 to 4 milliseconds. This means the 2-hop and 3-hop pulses will come down within the 5 mS Primary pulse length, resulting in superposition.

The Time Delays Between Multiple Modes are Less Than the Pulse Width. Therefore the Primary and Delayed Pulses Overlap, Lengthening the Pulse by Superposition.

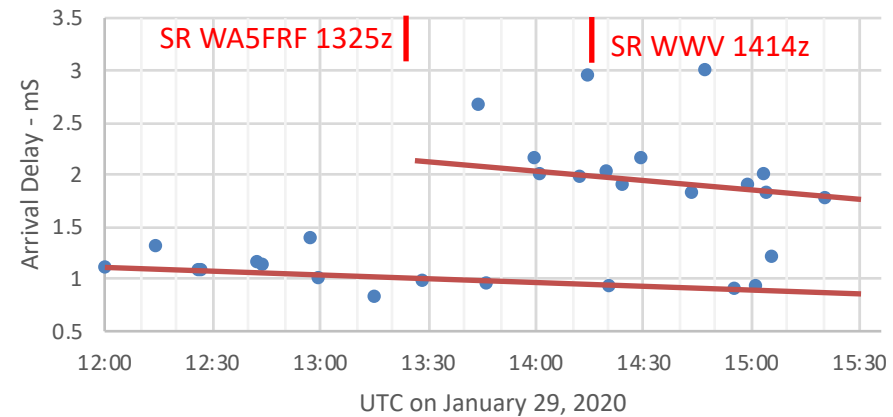


Timing data was extracted by measuring time delay from the GPSDO sync to the leading edge for the primary pulse and by the pulse extension on the trailing edge for the delayed pulses. Timing data was acquired over the 4 hour dawn transition on January 29, 2020.

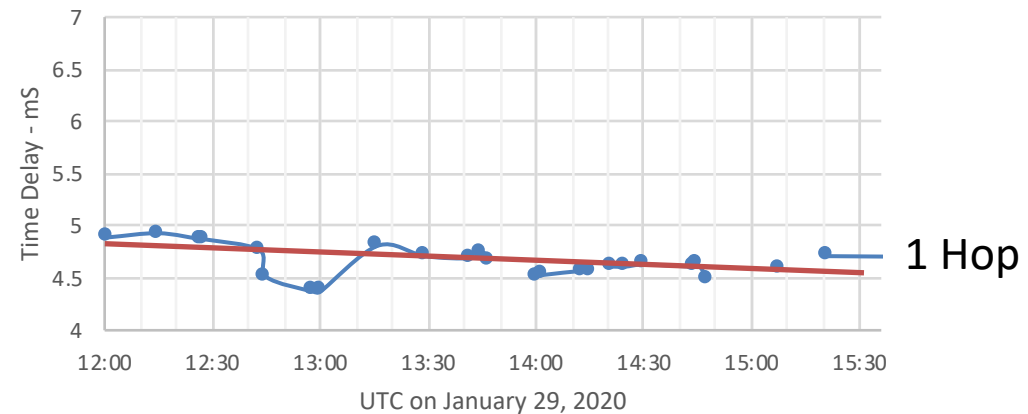
Scatter Plot of Primary and Delayed Pulses Clustered in Sequences Suggestive of Multiple Hop Modes

- Negative slopes are consistent with decreasing path lengths from descending ionization layer.
- Abrupt appearance of 3 Hop mode is consistent with spectrogram data and high angle propagation theory

Time Delay of Second, Third, and Fourth Pulses After Primary Pulse



Time from GPSDO Sync to 5 MHz Tick Arrival Corrected for 4.75mS Receiver DSP Delay

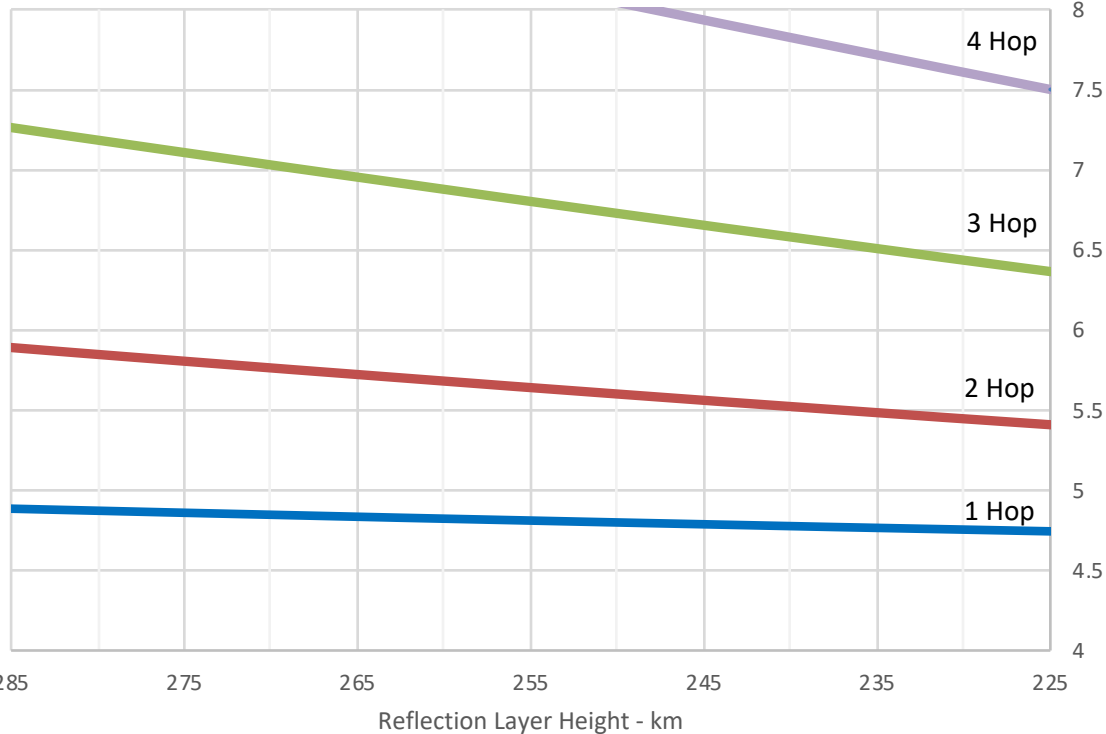


Actual arrival times of second and third delayed pulses can be estimated by adding the delay times in the top graph to the Primary arrival times in the bottom graph.

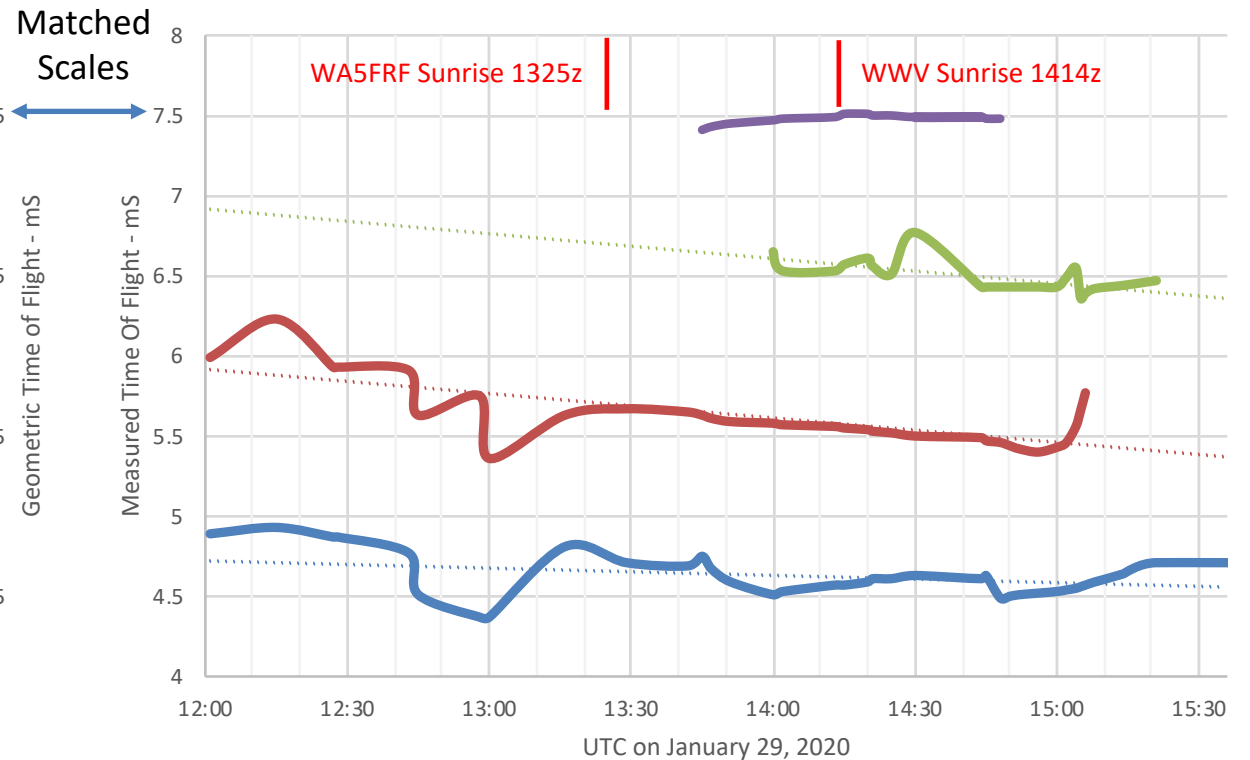
Effective virtual height descent rate available from slopes.

Measured TOF's were Consistent with Theoretical TOF's for a 255km Refraction Layer and Support Premise that Delayed Pulses Are from Multiple Hops

Geometric Time of Flight for 1, 2, 3, and 4 Hop Paths from WWV to WA5FRF vs. Reflection Layer Height



Measured and Interpolated TOF's from GPSDO Sync to Primary and Multiple Modes

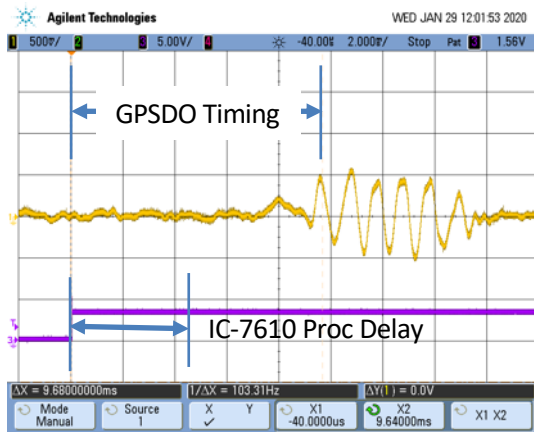


Geometric Times Of Flight plotted in descending order and cropped to approximately match measured data.

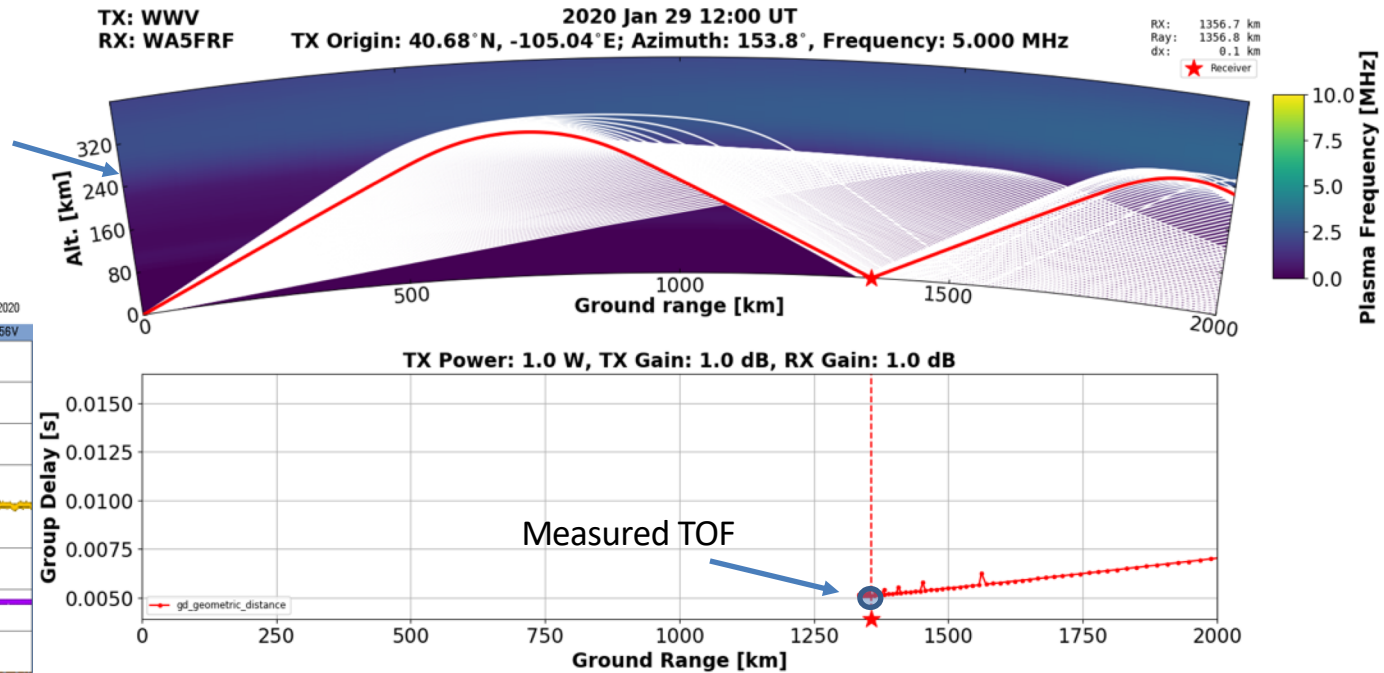
Measured 1-Hop Arrival Time is Consistent with Single Hop PHaRLAP Ray Trace Modeling

PHaRLAP Simulation Data Provided by Nathaniel Frissell W2NAF

Refraction height inferred from idealized geometry consistent PHaRLAP prediction.



Measured Data

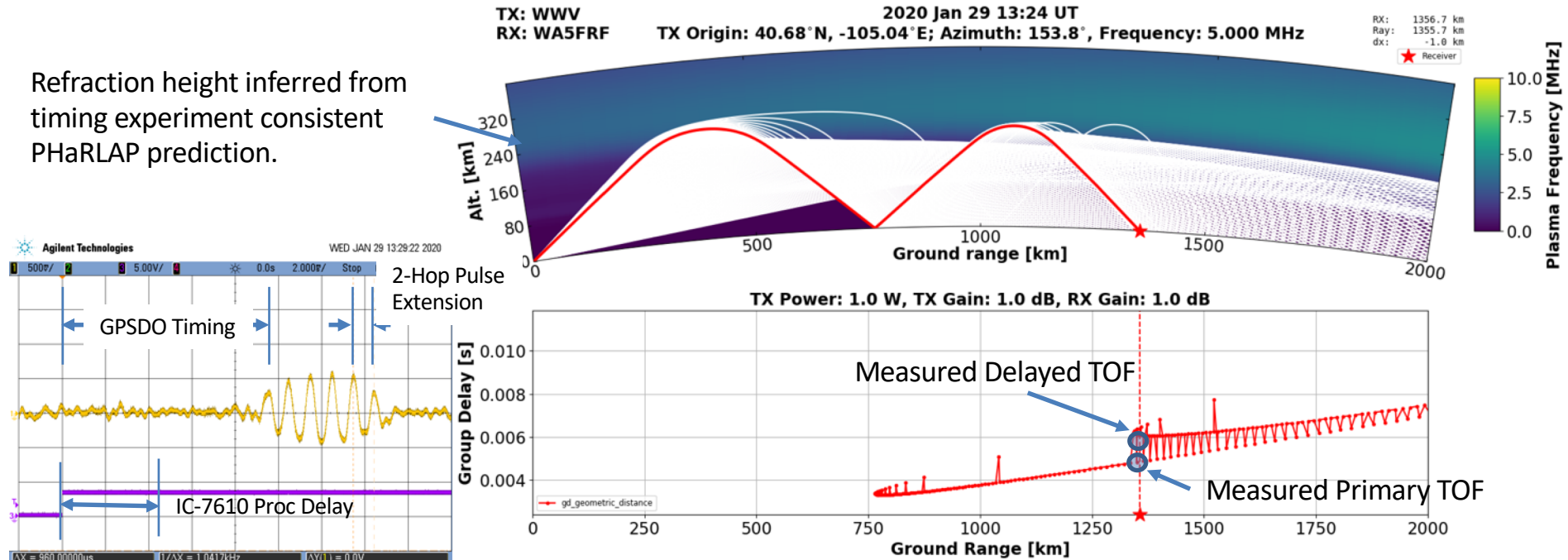


Predicted group delay near 5 mS consistent with measured arrival time of 4.93 mS for primary 1-hop mode at 1201z. $T = 9.68 \text{ (GPSDO)} - 4.75 \text{ (IC-7610)} = 4.93 \text{ mS}$.

Measured 2-Hop Arrival Time is Consistent with PHaRLAP Ray Trace Modeling

PHaRLAP Simulation Data Provided by Nathaniel Frissell W2NAF

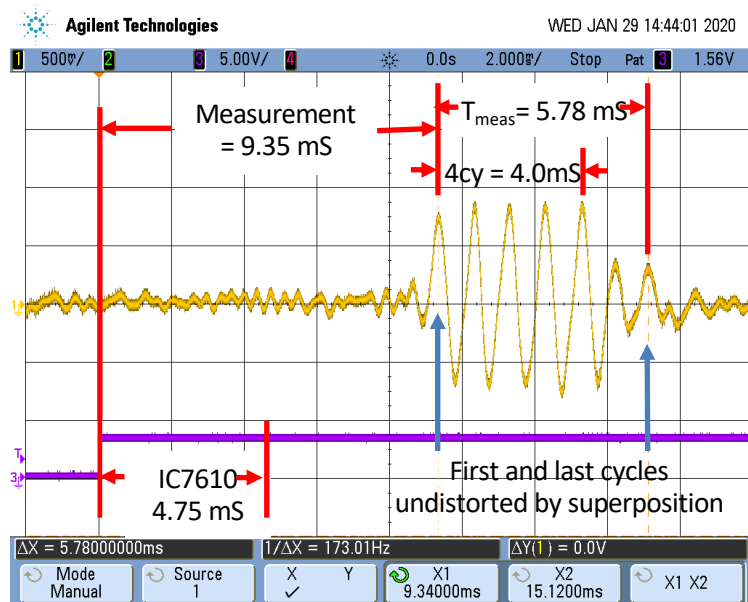
Refraction height inferred from timing experiment consistent PHaRLAP prediction.



Measured Data

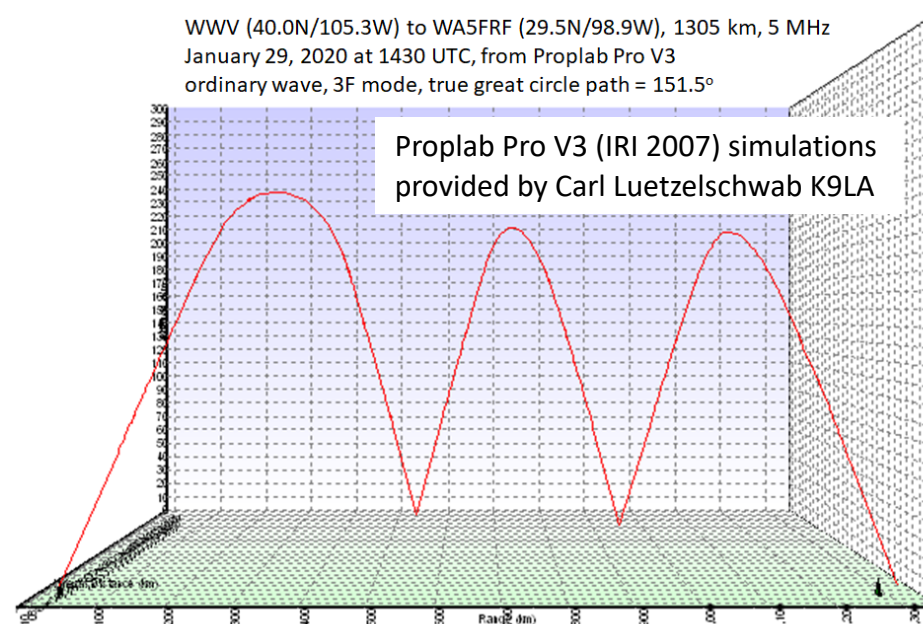
Predicted group delay near 6 mS consistent with measured 2-hop arrival time of 5.67 mS at 1329z. $T = 9.46 \text{ (GPSDO)} - 4.75 \text{ (IC-7610)} + 0.96 \text{ (Extension)} = 5.67 \text{ mS}$

Measured 3-Hop Arrival Time is Consistent with 3F Proplab Pro 3D Ray Trace Modeling



The best measurement technique is to reference the leading cycle of the primary and last cycle of the delayed pulses since they are not distorted by superposition.

WWV (40.0N/105.3W) to WA5FRF (29.5N/98.9W), 1305 km, 5 MHz
 January 29, 2020 at 1430 UTC, from Proplab Pro V3
 ordinary wave, 3F mode, true great circle path = 151.5°



$$\text{Measured 3F TOF} = \text{Leading Edge} - \text{IC7610} + T_{\text{meas}} - 4 \text{ cy} \\
 = 9.35 - 4.75 + 5.78 - 4.0 = 6.38 \text{ mS}$$

ray trace	mode	elev angle	az angle	total dist in km	time of flight assuming speed of light
3D	3F	49	143.3	1938	6.46 msec

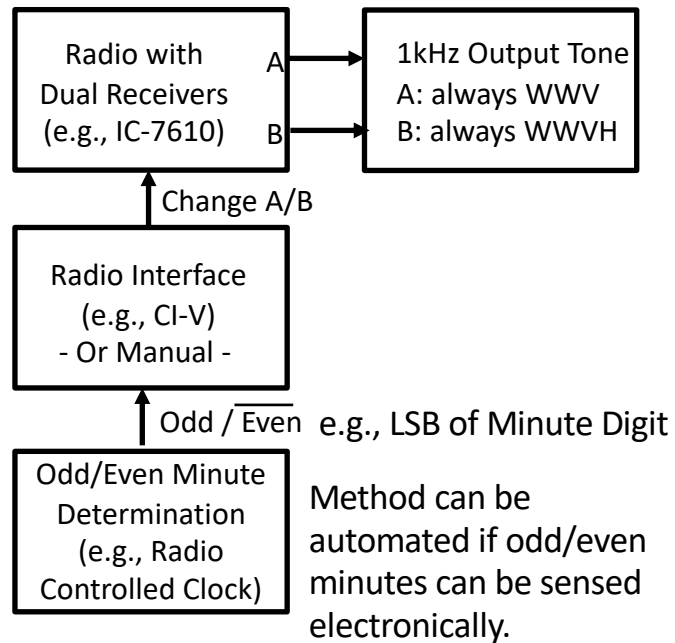
Separation of WWV and WWVH During Simultaneous Reception

- There are many times when the band is open to both WWV in Colorado and WWVH in Hawaii. Because they are on the same frequency the spectral contributions overlap in a spectrogram.
- WWV and WWVH alternately transmit standard side tones of 500 and 600 Hz on most (but not all) minutes of each hour. See <https://tf.nist.gov/stations/iform.html> . Their use as a separation tool was recognized by David Kazdan AD8Y.
- These signals are as precise as the carrier and can be used to separately measure Doppler data if recovered as an Upper Side Band (USB) tone.

<u>Minute</u>	<u>WWV</u>	<u>WWVH</u>
Even	500 Hz	600 Hz
Odd	600 Hz	500 Hz

Numerous separation schemes are possible using one or both tones. The option reported here is a fully deinterlaced technique that places 100% continuous data records for each station on separate outputs. The method requires two receivers with the ability to change frequency every minute so that one receiver continuously monitors WWV and the other WWVH. This method is also useful using only one programmable receiver to yield 100% data on just one station.

Deinterlace Scheme Using Dual (or Two) Receivers to Separate WWV and WWVH



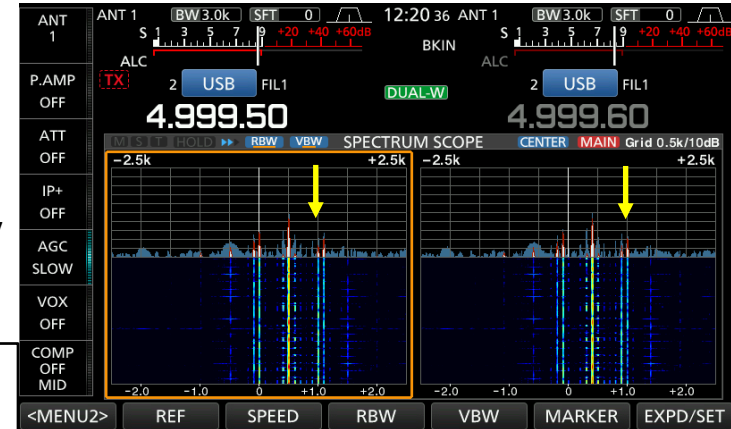
N.B. Scheme also works with a single receiver with programmable VFO or memory channels to output either WWV or WWVH alone.

Even minute:
MAIN on 500Hz for WWV
SUB on 600Hz for WWVH

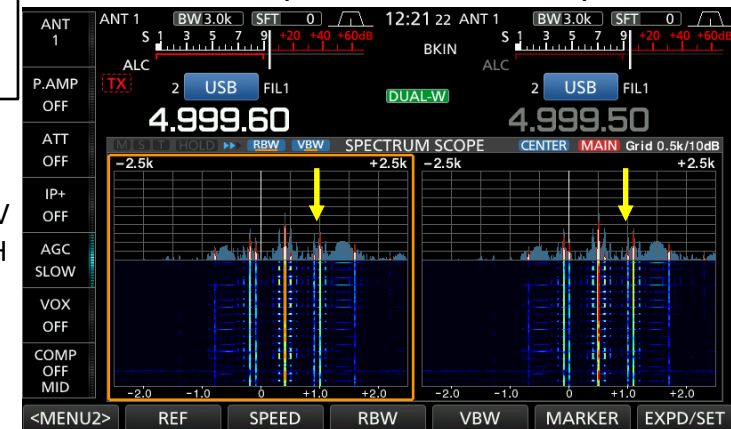
4.999.50 translates 500Hz USB to 1000Hz
4.999.60 translates 600Hz USB to 1000Hz

Odd minute:
MAIN on 600Hz for WWV
SUB on 500Hz for WWVH

MAIN = $f_c - 0.5$; SUB = $f_c - 0.4$; CHANGE every minute



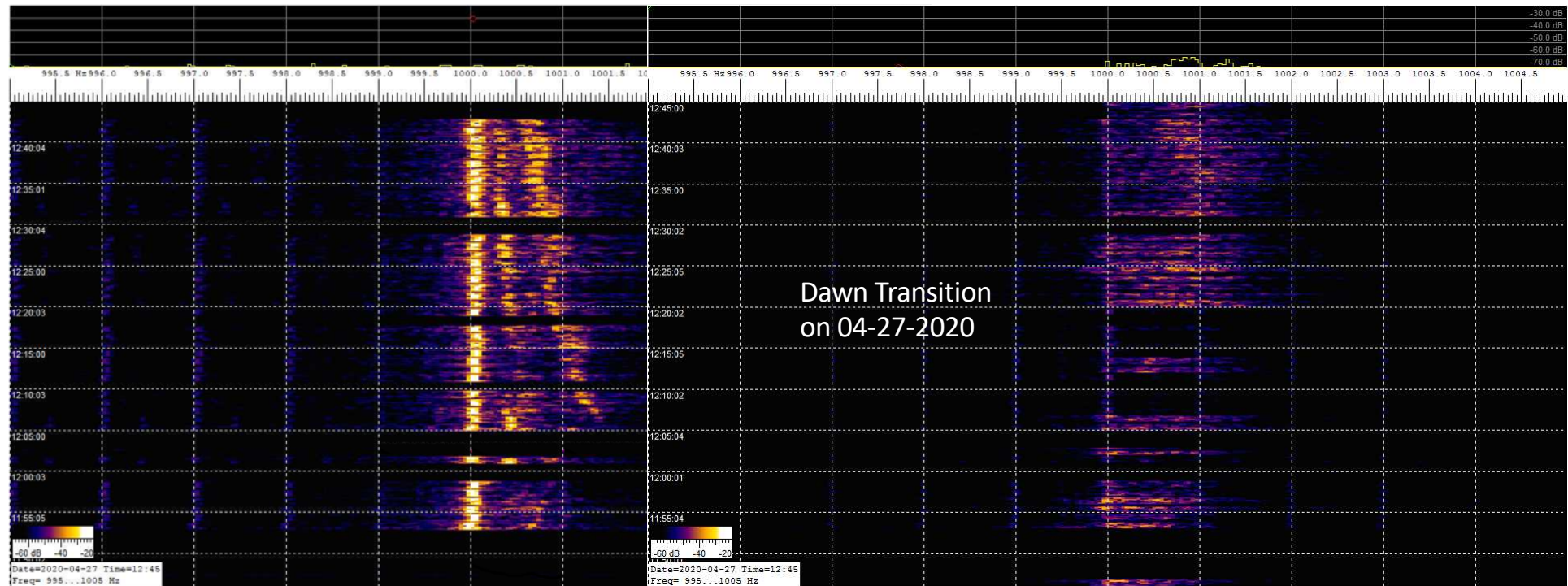
MAIN always WWV SUB always WWVH



IC-7610 screenshots in the two modes required to deinterlace the WWV/WWVH side tones. The radio was stabilized with a GPSDO.

Completely Deinterlaced WWV and WWVH Data

- IC-7610 Dual Receivers Using CHANGE to Manually Switch MAIN and SUB –
- Data is Present for Each Tone Every Minute It is On the Air -



Only WWV on MAIN
(Multiple Modes Present)

Only WWVH on SUB
(Single Mode Present)

Conclusions and Acknowledgements

- Using experimental tools targeting specific ionospheric behavior can help decipher the multiple physical processes involved. The purpose of this paper was to give examples of some of the tools developed for the HamSCI community.
- The results of the studies conducted to date support that at least some of the observed mode splitting may result from different Doppler shifts for multiple hop modes. But the data shows much more complexity than can be accounted for by this one mechanism. Alternate explanations have been proposed and are the subject of future research. An automated TOF data collection system with simultaneous spectrogram data would be of immense help.
- The author would like to thank Nathaniel Frissell W2NAF, Carl Luetzelschwab K9LA, David Kazdan AD8Y, Bill Liles NQ6Z, and Bill Engelke AB4EJ for their valuable insights and many excellent technical discussions.
- We gratefully acknowledge support to this project from NSF Grants AGS-2002278, AGS-1932997, and AGS-1932972